



HAL
open science

The brown seaweed *Cystoseira schiffneri* as a source of sodium alginate: Chemical and structural characterization, and antioxidant activities

Abdelkarim Benslimma, Sabrine Sellimi, Marwa Hamdi, Rim Nasri, Mourad Jridi, Didier Cot, S.M. Li, Moncef Nasri, Nacim Zouari

► To cite this version:

Abdelkarim Benslimma, Sabrine Sellimi, Marwa Hamdi, Rim Nasri, Mourad Jridi, et al.. The brown seaweed *Cystoseira schiffneri* as a source of sodium alginate: Chemical and structural characterization, and antioxidant activities. *Food Bioscience*, 2021, 40, pp.100873. 10.1016/j.fbio.2020.100873. hal-03369728

HAL Id: hal-03369728

<https://hal.science/hal-03369728v1>

Submitted on 7 Oct 2021

HAL is a multi-disciplinary open access archive for the deposit and dissemination of scientific research documents, whether they are published or not. The documents may come from teaching and research institutions in France or abroad, or from public or private research centers.

L'archive ouverte pluridisciplinaire **HAL**, est destinée au dépôt et à la diffusion de documents scientifiques de niveau recherche, publiés ou non, émanant des établissements d'enseignement et de recherche français ou étrangers, des laboratoires publics ou privés.

25 **Abstract**

26 Sodium alginates were extracted from brown seaweeds (*Cystoseira schiffneri*)
27 collected from a Tunisian island (Kerkennah, Sfax) in different seasons (December, April,
28 July and September). The structural features and antioxidant properties of *C. schiffneri*
29 sodium alginates (CSSA) were characterized. Micro-elementary analysis showed the absence
30 of nitrogen and sulfur in alginate fractions. All alginate isolates were high in uronic acids
31 (47.4-66.4%) and ash (24.3-39.4%). ATR-FTIR, NMR and circular dichroism data showed
32 that all CSSA were of the polyguluronate-type. Average molecular masses determined using
33 high performance size exclusion chromatography showed variations ranging from 4.49 to
34 1230 kDa. Thermogravimetric analysis suggested that CSSA were stable until 400°C except
35 for that collected in September, which was observed to only be stable until 200°C.
36 Antioxidant activity of CSSA from different seasons was measured using DPPH• radical-
37 scavenging, reducing power and Fe²⁺ chelating ability assays. Antioxidant potential of CSSA
38 varied significantly with respect to the season and the main factor controlling antioxidant
39 properties was the molecular mass.

40 **Keywords:** brown seaweed; *Cystoseira schiffneri*; sodium alginate; polyguluronate;
41 antioxidant activities.

42

43

44

45

46

47

48

49

50 **1. Introduction**

51 Seaweeds are known for their bioactive polysaccharides (Sanjeewa et al., 2017; Zhao
52 et al., 2018; Rengasamy et al., 2020). Algal polysaccharides are biodegradable, non-toxic and
53 biocompatible (Liu et al., 2015). Alginates are a family of linear copolymers containing
54 blocks of (1,4)-linked β -D-mannuronic acid (M) and α -L-guluronic acid (G) residues. Blocks
55 are composed of consecutive G residues or M residues or alternating M and G residues (Yang
56 et al., 2011). Structural features of alginates vary depending on species, season, geographic
57 location, among other parameters (Setyawidati et al., 2018). Alginates possess numerous
58 biological activities including antioxidant (Kumar et al., 2019; Sellimi et al., 2015),
59 antimicrobial(Li et al., 2017) and gastroprotective activities (Ammar et al., 2018). Their
60 biological properties are closely related to the proportion and distribution of M and G residues
61 as well as the molecular mass (MM).

62 Companies may use synthetic antioxidants, such as butylated hydroxyanisole (BHA)
63 and butylated hydroxytoluene (BHT) to control oxidation (Lorenzo et al., 2013). However,
64 the use of these synthetic compounds has been linked to carcinogenic effects
65 (KahlandKappus, 1993). Moreover, free radicals are the main cause of many diseases, such as
66 diabetes, cancer and neurodegenerative pathologies (Liu, 2020). A protection could occur
67 when free radicals were neutralized or trapped by antioxidant compounds (Schramm et al.,
68 2003). Naturally occurring antioxidants may be able to replace these synthetic compounds.

69 The brown seaweed *Cystoseira schiffneri*, collected from Kerkennah island during 4
70 seasons, was chosen as a natural matrix to extract and evaluate bioactive polysaccharides. The
71 annual cycle of the Mediterranean *Cystoseira* passes through a growth period between
72 February and May, a breeding period from June-July to August-September followed by a rest
73 period between October and December (Pellegrini et al., 1997). Hence, the current study aims

74 to assess the effect of seasonal variation on the structural features and antioxidant activities of
75 *C. schiffneri* sodium alginate (CSSA).

76 **2. Material and methods**

77 *2.1. Reagents*

78 1,1-Diphenyl-2-picrylhydrazyl (DPPH•), butylated hydroxyanisole (BHA), ethylene
79 diamine tetra-acetic acid (EDTA), 3-(2-pyridyl)-5,6-diphenyl-1,2,4-triazine-disulfonic acid
80 monosodium salt hydrate (ferrozine), Folin-Ciocalteu's reagent, phloroglucinol, glucose,
81 guluronic acid, sodium carbonate (Na₂CO₃), hydrochloric acid (HCl), ferrous chloride
82 (FeCl₂), 3,5 dimethylphenol, trichloroacetic acid (TCA), potassium ferrocyanide (C₆FeK₄N₆),
83 sulfuric acid (H₂SO₄), acetone, methanol, chloroform, 95% ethanol and other chemicals were
84 purchased from Sigma Chemical Co. (St. Louis, MO, USA).

85 *2.2. Sample collection and preparation*

86 The *Cystoseira schiffneri* samples were collected from Kerkennah islands (Tunisia)
87 around the point (34°39'30.07"N, 11°8'12.27"E) during low tide. Collections were done in
88 different seasons (December 2015, and April, July and September 2016). The identification of
89 collected seaweed was made by Pr. Asma Hamza from the National Institute of Marine
90 Science and Technology (Sfax, Tunisia). Seaweed fronds were washed with sea water to
91 eliminate impurities, and then transported to the laboratory in dark plastic bag for a period not
92 exceeding 12 h. Once arrived, seaweed fronds were washed with tap water followed by
93 distilled water to eliminate salts. After that, they were dried away from sunlight at room
94 temperature (25°C) for 20 days until reaching stable moisture. Dried fronds were ground
95 using a coffee grinder (Moulinex, Mayenne, France) and sieved through a 200 µm mesh size.
96 The powders were conserved at room temperature for a maximum of 8 wk in dried and sealed
97 dark glass containers.

98 2.3. *Sodium alginate extraction*

99 Crude sodium alginate extraction was done as previously described by Sellimi et al.
100 (2015). *C. schiffneri* powder (50 g) was defatted and depigmented using maceration twice (24
101 h, 30°C, 200 rpm) in acetone:methanol (7:3, v:v) (500 ml) followed by chloroform (300 ml).
102 Depigmented and defatted powder was air-dried, then demineralized by incubation (2 h,
103 60°C, 250 rpm) in 1 l 0.1 M HCl (pH 2). After cooling at room temperature, the residues were
104 recovered using centrifugation (20 min, 4000 ×g) in a Rotofix 32 centrifuge (Hettich,
105 Tuttlingen, Germany), washed with distilled water until neutral pH and then treated in 3%
106 Na₂CO₃ solution (pH11) for 2 h at 60°C and 250 rpm to solubilize alginate in the sodium salt
107 form. After centrifugation (20 min, 4000 ×g), the supernatant was recovered and two volumes
108 of absolute ethanol were added. Mixtures were left for 12 h at 4°C to precipitate sodium
109 alginate. The precipitated sodium alginate was suspended in distilled water and acidified
110 using 6 M HCl (pH 3) to allow gelation and thereby precipitation of alginate in its acidic
111 form. Precipitated alginic acids were recovered using centrifugation (20 min, 4000 ×g), then
112 suspended in distilled water and neutralized to pH 7.5 using 6 M NaOH. The crude sodium
113 alginate was precipitated using two volumes of absolute ethanol, dissolved again in distilled
114 water and lyophilized (Bioblock Scientific Christ ALPHA 1-2, IllKrich-Cedex, France). The
115 crude alginates extracted from *C. schiffneri* collected at December, April, July and September
116 were referred to AD AA AJ and AS, respectively.

117 2.4. *Chemical analysis*

118 The total sugars were determined using the method of Dubois et al. (1956). Briefly, to
119 0.3 ml CSSA solution (0.1 g/ml), 1 ml 5% phenol solution and 5 ml 12 NH₂SO₄ were added.
120 The mixture was incubated for 20 min at 30°C then the optical density was measured, using a
121 spectrophotometer (T70 UV-visible spectrometer PG Instruments Ltd., Lutterworth,
122 England), at 490 nm against a standard curve prepared using glucose.

123 The uronic acids (U) were determined using the method of Scott (1979). To 0.3 ml
124 CSSA solution (0.1 g/ml), 5 ml 12 N H₂SO₄ and 0.3 ml of a solution containing 20 g/l NaCl
125 and 30 g/l H₃BO₃ were added. The mixture was incubated at 70°C for 40 min, then cooled to
126 room temperature for 1 h before adding 0.2 ml 3,5-dimethylphenol. After 10 min at room
127 temperature, the absorbance was measured at 400 and 450 nm against a standard curve of
128 galacturonic acid. U (%) were calculated using equation 1.

$$129 \quad U (\%) = (\Delta A \times V \times D \times C_s \times 0.91 \times 100) / (\Delta A_s \times m)(1)$$

130 Where ΔA = the difference in absorbance, V = the total solution volume (ml), D = the
131 sample dilution, C_s = the standard concentration, ΔA_s = the difference in the absorbance of
132 the standard (100 µg/ml), m = the mass of the test sample (mg), and 0.91 is the conversion
133 factor of the experimental determination of monosaccharides to polysaccharides.

134 Total phenolics were determined using slightly modified methods described by Cicco
135 et al. (2009). Phloroglucinol was used as the standard. Briefly, 100 µl of sample solution (2
136 mg/ml) was mixed with 100 µl 2 N Folin-Ciocalteu's reagent and 800 µl 5% Na₂CO₃ solution.
137 The mixture was incubated at 40°C for 20 min, then absorbancies were measured at 760 nm
138 against a standard curve of phloroglucinol.

139 *2.5. Micro-elementary analysis*

140 Elemental composition of CSSA was done using an EDX analyzer (X-Max^N SDD
141 EDX Instrument, Oxford, UK). Results were treated using Oxford AZTEC software 2011
142 (Oxford Instruments, Abingdon, UK). The samples were metalized previous to analyses using
143 a Quorum Technologies metalizer (Quorum Technologies, Guelph, ONT, Canada).

144 *2.6. Circular dichroism*

145 A Jasco J-815 CD spectrometer (Jasco Corp., Tokyo, Japan) was used to obtain
146 circular dichroism spectrum in the range of 190-260 nm. The sample solution was at a
147 concentration of 0.25 mg/ml. A circular dichroism spectrum is often reported in ellipticity

148 degrees (θ) expressed as milli-degrees. The ratio of peak height to trough depth was
149 calculated using equation 2 (Morris et al., 1980).

150
$$\text{Peak/trough ratio} = (q_{\text{trough}} - q_{\text{peak}})/q_{\text{trough}}(2)$$

151 *2.7. ATR-FTIR spectroscopy*

152 Attenuated total reflectance (ATR)-Fourier transform infrared (FTIR) spectra of CSSA
153 were obtained in the range of 4000–600 cm^{-1} at room temperature using 30 scans and 4 cm^{-1}
154 resolution. A FTIR Spectrum 100 spectrometer (Perkin-Elmer, Norwalk, CT, USA) with ATR
155 accessory containing a diamond/ZnSe crystal was used to obtain infrared spectrums.

156 *2.8. NMR spectroscopy analysis*

157 ^1H -NMR spectra were obtained using a Bruker 300 spectrometer (Bruker Biospin AG,
158 Fallanden, Switzerland) at 60°C. Results were treated using Mestre Nova (MNOVA) software
159 version 5.3.0 (Mestrelab Research S.L., Santiago de Compostela, Spain). Samples were
160 deuterium-exchanged using lyophilization with D_2O and then studied as 1% (m/v) solutions in
161 D_2O (99.96%). Signals in the anomeric region (4.4-5.1 ppm) were studied to determine the
162 CSSA structure. Therefore, F_M , F_G , F_{GG} , F_{MM} , F_{GM} and F_{MG} blocks of CSSA were calculated
163 based on the areas of signals (I), (II) and (III) (Fertah et al., 2017) and using equations 3, 4,5,
164 6 and 7. In addition, M/G ratio can be calculated based on the equation 8.

165
$$F_G = A_I / (A_{II} + A_{III}) \quad (3)$$

166
$$F_M = 1 - F_G(4)$$

167
$$F_{GG} = A_{III} / (A_{II} + A_{III}) \quad (5)$$

168
$$F_{MG} = F_{GM} = F_G - F_{GG}(6)$$

169
$$F_{MM} = F_M - F_{MG}(7)$$

170
$$M/G = F_M / F_G(8)$$

171 2.9. *MM distribution*

172 The number-average molecular mass (M_n), the average molecular mass (M) and
173 polydispersity index (PDI) of CSSA were determined using a Waters Alliance model
174 GPCV2000 (Waters, Milford, MA, USA). High performance size exclusion chromatography
175 (HPSEC) equipped with a multi-angle laser light scattering (MALLS) detector from Wyatt
176 (Wyatt Technology, Santa Barbara, CA, USA). Before injection, the apparatus was calibrated
177 with toluene and normalized with a solution of polyethylene oxide (72 kDa) in 0.1 M NaCl
178 and the samples were filtered through a 0.45 μm pore size membrane (Merck, Darmstadt,
179 Germany). The sample (100 μl) of 3 mg/ml was injected in a column TSK-G2000 SWXL (7.8
180 \times 300 mm). Elution was carried out at 25°C using 0.1 M NaCl as eluent at a flow rate of 0.5
181 ml/min. The refractive index increment (dn/dc) was 0.155. Data collected from the refractive
182 index detector (RID) and MALLS were treated using ASTRA software version 4.72.03
183 (Wyatt Technology, Goleta, CA, USA).

184 2.10. *Thermogravimetric analyses*

185 Thermogravimetric analyses (TGA) of the extracted sodium alginates were done on a
186 TGA Q500 instrument (TA Instruments, Newcastle, DE, USA). Nitrogen flow rate was 60
187 ml/min and the temperature increase from 20 to 1000°C by 20°C/min.

188 2.11. *Rheological analysis*

189 Rheological analyses of sodium alginates solutions (3%,m/v) from different seasons
190 were done on a Physica MCR 301 rheometer (Anton-Paar GmbH, Graz, Austria) using the
191 dispositive plan-plan 50 with a measurement gap of 0.1 mm and temperature of 20°C.
192 Viscosity was measured as a function of shear rate (0.1-100 s^{-1}). Storage modulus (G') and
193 loss modulus (G'') were measured as a function of frequency (2-100 Hz).

194 2.12. *Antioxidant activity*

195 2.12.1. *DPPH• radical-scavenging activity*

196 Radical-scavenging activity was measured as described by Kirby and Schmidt(1997)
197 with slight modifications. Sample solutions were prepared at different concentrations from
198 0.125 to 1.5 mg/ml. In each tube, 500 µl of the sample solution was reacted with 375 µl of
199 ethanol solution and 125 µl of DPPH• solution (0.2 mM in ethanol) as the free radical source.
200 The reaction mixtures were incubated for 60 min in the dark at room temperature and the
201 reduction of DPPH• radical was measured at 517 nm. Control (without sample) and blanks
202 (without DPPH•) were prepared. Results of DPPH• scavenging activity are shown as IC₅₀
203 values (µg/ml), defined as the extract concentration needed to scavenge 50% DPPH•.

204 2.12.2. *Reducing power*

205 Ferrous reducing activity was measured as previously described by Yildirim et al.
206 (2001). Sample solutions were prepared at different concentrations from 50 to 500 µg/ml.
207 Sample solution (0.5 ml) was added to 1.25 ml 0.2 M sodium phosphate buffer (pH 6.6) and
208 1.25 ml 1% (m/v) potassium ferrocyanide. Mixtures were incubated for 30 min at 50°C. After
209 incubation, 1.25 ml 10% (m:v) TCA was added and the mixture was centrifuged at 11000 ×g
210 for 10 min. From each supernatant, 1.25 ml was transferred and diluted with 1.25 ml ultrapure
211 water. Finally, FeCl₃ (250 µl) were added and absorbancies were measured at 700 nm after 10
212 min incubation at room temperature. Blanks without FeCl₃ were prepared for each
213 concentration. The reducing power is shown as the extract concentration (EC_{0.5}) providing 0.5
214 absorbance at 700 nm.

215 2.12.3. *Fe²⁺ chelating ability*

216 The CSSA capacity to complex ferric ions were measured using the method reported
217 by Carter (1971). Sample solutions were prepared at different concentrations from 0.1 to 1
218 mg/ml. Briefly, 100 µl of sample solution, 50 µl 2 mM FeCl₂ and 450 µl distilled water were

219 mixed and incubated for 3 min at room temperature. Volumes of 200 μ l 5 mM ferrozine were
220 added and mixtures were incubated again at room temperature for 10 min before measuring
221 absorbancies at 562 nm. Blanks without ferrozine and control without sample were prepared.
222 Results of metal (Fe^{2+}) chelating ability are shown by IC_{50} values ($\mu\text{g/ml}$), defined as the
223 extract concentration needed to chelate 50% Fe^{2+} .

224 2.13. Statistical analysis

225 All analytical determinations were done in triplicate. One-way analysis of variance
226 (ANOVA) was done using the statistical package for the social sciences (SPSS) software for
227 Windows™ (version 17, SPSS Inc., Chicago, IL, USA). Duncan's multiple range tests
228 ($p < 0.05$) was used to compare the average responses between samples.

229 3. Results and discussion

230 3.1. Extraction yield

231 The extraction yields of CSSA from different seasons are shown in Table 1. Extraction
232 yield of AJ was higher than AA and AD. While, AS showed the lowest extraction yield. The
233 results were comparable to those reported for *Dictyota dichotoma* (20.9%), *Padina*
234 *boergeseni* (24.3%) and *Sargassum tenerrimum* (32.6%) (Parthiban et al., 2012), but
235 significantly higher than those of *D. caribaea* (7.4%) and *P. perindusiata* (5.4%) (García-Ríos
236 et al., 2012). Alginate extraction yield is dependent on the season and thereby the
237 development stage of *C. schiffneri*. Kumar and Sahoo (2017) reported that the highest alginate
238 yield from *S. wightii* was obtained in March (32%), however, the lowest one (24%) was
239 obtained in July. Setyawidati et al. (2018) described that extraction yields of alginate from *S.*
240 *aquifolium* were higher during the dry season (May, June) (39%) than during the wet season
241 (November) (24%). On the other hand, *P. boryana* showed extraction yields of 9% during the
242 wet season against 6% during the dry season. Therefore, the seasonal variation of alginate
243 yield did not follow one trend line for all species.

244 3.2. *Chemical analysis*

245 Moisture, ash, total phenolics, total sugars and U of CSSA from different seasons are
246 shown in Table 1. High amounts of U and ash were observed for all seasons, while markedly
247 low amounts of total sugars were measured. However, traces of phenolic compounds were
248 found. U and neutral sugars of CSSA were comparable to those of *C. barbata* alginate (58.1
249 and 9.3%, respectively) (Sellimi et al., 2015). Similarly, Ammar et al. (2018) showed that U
250 are ~ 60% for three species *C.compressa*, *P. pavonica* and *Dictyopteris*
251 *membranacea*. Similarly, alginate isolated from *C. compressa* had traces of phenolic
252 compounds (1.11%) (Hentati et al., 2018). Standard alginates also showed the presence of
253 impurities. Dusseault et al. (2006) detect proteins (5.9 mg/g) and polyphenols (13.8 AFU) in
254 food-grade sodium alginate.

255 3.3. *Elementary analysis*

256 The elemental composition of CSSA from all seasons is shown in Table 1. High levels
257 of carbon, oxygen and sodium while low contents of Mg, Cl, Si and K were measured. Sulfur
258 and nitrogen were not found, which indicated the absence of proteins and fucans in the
259 extracted alginates. Elementary analysis therefore suggested that CSSA fractions occurred as
260 a sequence of U linked predominately to sodium ions.

261 3.4. *FTIR spectroscopy*

262 Fig. 1. shows the spectral data relative to the ATR-FTIR spectroscopy analysis of the
263 CSSA fractions. The bands at 3354 and 2935 cm^{-1} were assigned to O–H and C–H stretching
264 vibrations, respectively (Hentati et al., 2018). Signals at 1605 and 1423 cm^{-1} were attributed,
265 respectively to asymmetric and symmetric C=O stretching vibrations. The band at 1025 cm^{-1}
266 assigned to C-O-C of glycosidic linkage was the polysaccharides characteristic band (Hentati
267 et al., 2018). The bands, in the anomeric region (750-950 cm^{-1}), were assigned to U residues
268 (Chandía, 2001; Chandía et al., 2004). The peak ratio at 1125 and 1025 cm^{-1} allows the

269 estimation of M/G ratio (Gómez Ordóñez and RupérezAntón, 2011). Overall, the estimated
270 M/G ratios of CSSA for the 4 seasons ranged between 0.062 and 0.065 (Table 2), which
271 suggest that all CSSA were of the polyguluronate-type.

272 3.5. Circular dichroism

273 The M/G ratios of sodium alginate fractions could also be determined from circular
274 dichroism spectra based on the empirical correlation between the peak (~195 nm) to depth
275 (~205 nm) ratio (Morris et al., 1980). The CSSA spectra showed that peaks ~195 nm were
276 almost absent for all samples (Fig. 2). Therefore, the calculated M/G ratios did not exceed
277 0.022 (Table 2). The CSSA fractions were, therefore, composed essentially by G residues,
278 which confirmed the FTIR data. Ramos et al. (2018) reported that low M/G ratio of alginates
279 resulted in strong and big gels with interactions with calcium ions. The CSSA fractions seem
280 to be interesting for strong gels applications and this during all algae development stages.

281 3.6. MM distribution

282 MM distributions of CSSA were determined and results are shown in Table 3. For all
283 seasons, the CSSA fractions were polydisperse (PDI>1). The polydispersity may be due to the
284 use of the whole thalli. Handå et al. (2013) reported that alginate MM varied as a function of
285 the thalli part. Hence, the MM of alginate was an average over the whole distribution.

286 The highest MM was obtained for AD, followed by AJ, AA and AS. The AA and AJ
287 fractions had MM comparable to commercial sodium alginates CR8133 (M = 90-180 kDa)
288 and CR8223 (M= 250-350 kDa), respectively (Ramos et al., 2018). MM of CSSA for all the
289 seasons, except for December, were observed to be lower than those of sodium alginates
290 extracted from 8 species of *Saccharina* (511-616 kDa) (Suzuki et al., 2016).

291 The important variation noted between seasons for MM may be related to the life
292 cycle of *C. schiffneri*. In December at the rest period thalli are formed entirely of old stems
293 characterized by high MM. In April, during the growth period new stems with low MM

294 appear on old stems and continue growing gaining higher MM. In September, after
295 reproduction it appears new thalli formed entirely by the new stems that are characterized by
296 low MM (Handå et al., 2013)

297 *3.7. NMR spectroscopy analysis*

298 ¹H-NMR spectra of CSSA from the different seasons are shown in Fig. 3. Characteristic
299 bands were observed to be around 1.5, 2.0, 4.5, 5.0 and 5.5 ppm for all the seasons. The
300 distribution of M and G could be studied based on signals from the anomeric region (Fertah et
301 al., 2017). Signal (I) that correspond to G-1 anomeric proton of G was obtained at 5.35 ppm.
302 Signal (II), that was due to the overlap between the M anomeric proton (M-1) and the C-5 of
303 the alternating blocks (GM-5), was obtained at 4.93 ppm. Similarly, signal (III) characterizing
304 H-5 G proton (GG-5G) was obtained at 4.84 ppm. The calculated F_G , F_M , F_{GG} , F_{MM} , F_{MG} and
305 F_{GM} are shown in Table 4. The results of the calculated M/G ratios (Table 2) were consistent
306 with the circular dichroism and FTIR spectroscopy data, in which the CSSA fractions were
307 defined as polyguluronates. Higher M/G ratios were described by Mohammed et al. (2020)
308 (M/G=0.45), Okolie et al.(2020) (M/G=0.87), Davis et al. (2003) (M/G=0.19) and Larsen et
309 al. (2003) (M/G=0.45). There were no previous studies describing comparable or lower M/G
310 ratios. The CSSA fractions might be the first reported as polyguluronates. The results for
311 structural composition showed through the year high F_G and F_{GG} values and low F_M , F_{MM} and
312 F_{MG} values. These results suggested that CSSA fractions were composed essentially by G
313 blocks punctuated with low amounts of M and MG blocks. Gelling properties of alginate are
314 related to G blocks responsible for the “Egg Box” structure (Xiao et al., 2015). High F_{GG}
315 values for CSSA fractions with high M/G ratio suggested the possibility to form a strong and
316 rigid gel.

317 Results for the M/G ratio determined using three methods suggested that through the
318 year the CSSA fractions were of the polyguluronate-type with low amounts of M. However,

319 the values obtained from one method to another. Hence, it should be pointed out that the M/G
320 ratio calculated from FTIR spectra were only an approximation. The circular dichroism,
321 which determines the ratio of M to G based on empirical correlation, gives more accurate
322 results. Overall, NMR spectra gave the best calculations not only for the M/G ratio but also
323 for GGG, MGM, MG, MM, GGM and MGG. Hence, Hentati et al.(2018) reported that NMR
324 is the only reliable and accurate method to study the alginate structure.

325 *3.8. Thermogravimetric analysis*

326 The mass losses of CSSA from the 4 seasons as function of temperature are shown in
327 Fig. 4. Idris et al. (2012) reported that the combustion had three phases namely drying (50-
328 220°C), pyrolysis (220-500°C) and char combustion (>500°C). The first mass loss was
329 attributed to the evaporation of non-bonded water and it occurred between 50 and 150°C
330 (Mallick et al., 2018). The second mass loss, between 150 and 220°C, was assigned to the loss
331 of bonded water. Fig. 4 shows that the most important mass loss was observed around 400°C
332 for all CSSA fractions, except for AS (around 200°C), which was due to the degradation of
333 the osidic monomers. The decrease of temperature degradation of AS compared to others
334 alginates could be related to their lower MM. Mallick et al. (2018) reported that low MM
335 molecules had high volatility and could therefore accelerate degradation. Differences among
336 seasons could be explained by the MM differences and the presence of minerals. López-
337 González et al. (2014) reported that alkali metals catalyzed combustion that was characterized
338 by multiple and small mass losses.

339 *3.9. Rheological properties*

340 *3.9.1 Rotational analysis*

341 The viscosities of AA, AJ and AS decreased with shear rates indicating a shear-
342 thinning behaviors (Fig. 5). However, Newtonian behavior was observed for AD at shear rates
343 $>10 \text{ s}^{-1}$ indicating that the CSSA flow has encountered more resistance at high shear rate

344 (Benchabane and Bekkour, 2008). Comparable viscosities were observed for all the seasons
345 except for AD that showed low viscosity. The difference of AD behavior from other CSSA
346 fractions might be related to its higher MM giving more intermolecular entanglements.
347 Comparable results were shown by Rezende et al. (2009) for alginate showing shear-thinning
348 behaviors. Hentati et al. (2020) reported that at low concentrations (0.25-2%) of *C. compressa*
349 alginate, shear-thinning behavior was observed at low shear-rates that turn to Newtonian
350 behavior at high shear-rates. However, at high concentrations (3-5%) only shear-thinning
351 behaviors were shown. The shear-thinning behavior observed for the CSSA fractions
352 facilitates the flow compared with a Newtonian fluid allowing high flow rates for equal
353 pressures (Rezende et al., 2009).

354 *3.9.2. Oscillatory analysis*

355 The increase in G' for AD with increasing frequencies suggested that elastic behavior
356 becomes dominant (Fig. 6). However, for AA, AJ and AS, G' remained almost constant with
357 the increase of frequency indicating no elastic behavior for alginate solutions (Böhning et al.,
358 2019). All samples showed viscous liquid-like behavior as the G'' values were greater than
359 the G' for all the samples (Hentati et al., 2020). The elastic behavior of AD seemed to be due
360 to the high MM. However, the CSSA from other seasons should be considered as non-viscous
361 liquids, which could be important for some manufacturing uses (Rezende et al., 2009).

362 *3.10. Antioxidant activity*

363 *3.10.1. DPPH• radical-scavenging ability*

364 The DPPH• radical-scavenging test reflects the ability of a sample to stabilize free
365 radicals by donating a proton. Fig. 7 shows the concentration dependent radical-scavenging
366 activity of CSSA and the IC_{50} values are shown in Table 5. The AS with the lowest MM
367 showed the lowest IC_{50} value and therefore the best activity. However, radical-scavenging
368 activity of CSSA remained lower than that of BHA. Overall, the CSSA fractions were

369 observed to show higher antiradical activity than alginate hydrolysates ($IC_{50}=10.4$ mg/ml)
370 (Zhu et al., 2016). However, Hentati et al. (2018) reported that *C. compressa* sodium alginate
371 with MM of 1.105 g/mol had higher activity ($IC_{50} = 560$ μ g/ml) than those of AD, AA and
372 AJ, but remained lower than that of AS. A positive correlation between radical-scavenging
373 activity at 1500 μ g/ml and MM ($R^2=0.31$) was observed. Therefore, the main factor
374 controlling the antioxidant properties of sodium alginates seems to be the MM. Accordingly,
375 Kelishomi et al. (2016) showed that radical-scavenging activity of alginates was inversely
376 proportional to the MM. Higher MM polysaccharides had a more compact structure, resulting
377 in stronger intramolecular hydrogen bonds and thus restricting the hydrogen groups.
378 Therefore, the access of active groups to oxidant molecules is more difficult.

379 3.10.2. Reducing power

380 The ability of CSSA to stabilize oxidants by donating an electron was measured and
381 results are shown in Fig. 7. The CSSA fractions showed a reducing power in a concentration-
382 dependent manner and the $EC_{0.5}$ values are shown in Table 5. The highest activities were
383 obtained for AS and AD followed by AJ. However, the $EC_{0.5}$ values of CSSA from all seasons
384 remained lower than that of BHA. All CSSA fractions, except AA, showed higher reducing
385 power than that of *C. barbata* sodium alginate (absorbance of 0.7 at 0.5 mg/ml) (Sellimi et al.,
386 2015). Comparable results to AJ were reported for *C. compressa* sodium alginate that showed
387 absorbance ~ 1 at 0.5 mg/ml (Hentati et al., 2018). The reducing power of polysaccharides
388 was directly related to their MM and to the hydroxyl and carboxyl groups of U (Raza et al.,
389 2011; Shang et al., 2018). However, the present study showed contradictory results, where the
390 reducing abilities of CSSA fractions were not correlated with either their MM or their U.
391 However, inconsistent results were also described by others. Cheng et al. (2013) indicated that
392 polysaccharide fractions from *Epimedium acuminatum* with high MM had high antioxidant
393 activity. Kardošová and Machová (2006) reported that for some polysaccharides and

394 oligosaccharides the MM was not correlated with the antioxidant levels. Hence, the MM-
395 antioxidant activity relation of alginate is still uncertain.

396 3.10.3. Fe^{2+} chelating ability

397 The chelating abilities of CSSA was dependent on the concentration and the results are
398 shown in Fig. 7, and the IC_{50} values are shown in Table 5. The highest activity was obtained
399 for AS followed by AD and AJ, while the lowest Fe^{2+} chelating ability was measured for AA.
400 Nevertheless, the CSSA from all the samples showed lower chelating abilities than EDTA.
401 The AS, which had the lowest MM, had the highest Fe^{2+} chelating ability. These results were
402 consistent with the results of Wang et al. (2016) who reported that the Fe^{2+} chelating ability of
403 polysaccharides decreased with increased MM. However, AD with higher MM showed higher
404 chelating ability. Similarly, Cheng et al. (2013) reported that polysaccharide fractions from
405 *Epimedium acuminatum* with high MM had more antioxidant activity. Kardosová and
406 Machová (2006) showed that MM of some polysaccharides and oligosaccharides was not
407 significantly related to the antioxidant properties. The chelating ability was mostly due to OH,
408 -COOH, -C=O and -O-groups (Wang et al., 2016). The relationships between antioxidant
409 activity and physico-chemical properties or structural features have not been comprehensively
410 elucidated and confirmed. Conflicting results have been observed in the literature. Extraction
411 source and methods, and even drying procedures can influence the results. Furthermore, other
412 antioxidant substances, such as polyphenol may be retained in polysaccharides fractions and
413 should be taken into account. Overall, the antioxidant potential of polysaccharides is not
414 determined by a single factor but a combination of several related ones (Wang et al., 2016).

415 4. Conclusion

416 The seasonal variation effect on structural features and antioxidant activities of sodium
417 alginate extracted from *C. schiffneri* (CSSA) was studied. The isolated alginates fractions
418 were of the polyguluronate-type and most of them were stable until 400°C. The CSSA

419 showed season-dependent structural characteristics and antioxidant activities. The techno-
420 functional properties of the CSSA should be studied and compared to commercial alginates.
421 The CSSA might be used in a variety of applications including food and biomedical
422 formulations.

423 **Acknowledgments**

424 Financial assistance for this study was provided by the Ministry of Higher Education
425 and Scientific Research, Tunisia and supported by the Utique-PHC program (project
426 SEAPOLYMERHYDROGEL) N° 19G0815 of the CMCU funded by the Ministry of Higher
427 Education and Scientific Research, Tunisia.

428 **Conflicts of interest**

429 The authors confirm that they have no conflicts of interest with respect to the study
430 described in this manuscript.

431 **References**

- 432 Ammar, H. H., Lajili, S., Sakly, N., Cherif, D., Rihouey, C., Le Cerf, D., Bouraoui, A.,
433 &Majdoub, H. (2018). Influence of the uronic acid composition on the
434 gastroprotective activity of alginates from three different genus of Tunisian brown
435 algae. *Food Chemistry*, 239, 165–171.
436 <https://doi.org/10.1016/j.foodchem.2017.06.108>
- 437
- 438 Benchabane, A., &Bekkour, K. (2008). Rheological properties of carboxymethyl cellulose
439 (CMC) solutions. *Colloid and Polymer Science*, 286(10), 1173.
440 <https://doi.org/10.1007/s00396-008-1882-2>
- 441 Böhning, M., Frasca, D., Schulze, D., &Schartel, B. (2019). Multilayer graphene/elastomer
442 nanocomposites. In S. Yaragalla, R. K. Mishra, S. Thomas, N. Kalarikkal, & H. J.
443 Maria (Eds.), *Carbon-Based Nanofillers and Their Rubber Nanocomposites*. New
444 York:Elsevier. p 139–200.<https://doi.org/10.1016/B978-0-12-817342-8.00006-8>

445 Carter, P. (1971). Spectrophotometric determination of serum iron at the submicrogram level
446 with a new reagent (ferrozine). *Analytical Biochemistry*, 40(2), 450–458.
447 [https://doi.org/10.1016/0003-2697\(71\)90405-2](https://doi.org/10.1016/0003-2697(71)90405-2)

448 Chandía, N. (2001). Alginic acids in *Lessoniatrabeculata*: Characterization by formic acid
449 hydrolysis and FT-IR spectroscopy. *Carbohydrate Polymers*, 46(1), 81–87.
450 [https://doi.org/10.1016/s0144-8617\(00\)00286-1](https://doi.org/10.1016/s0144-8617(00)00286-1)

451 Chandía, N. P., Matsuhira, B., Mejías, E., & Moenne, A. (2004). Alginic acids in
452 *Lessoniavadosa*: Partial hydrolysis and elicitor properties of the polymannuronic acid
453 fraction. *Journal of Applied Phycology*, 16(2), 127–133.
454 <https://doi.org/10.1023/B:JAPH.0000044778.44193.a8>

455 Cheng, H., Feng, S., Shen, S., Zhang, L., Yang, R., Zhou, Y., & Ding, C. (2013). Extraction,
456 antioxidant and antimicrobial activities of *Epimediumacuminatum* Franch.
457 polysaccharide. *Carbohydrate Polymers*, 96(1), 101–108.
458 <https://doi.org/10.1016/j.carbpol.2013.03.072>

459 Cicco, N., Lanorte, M. T., Paraggio, M., Viggiano, M., & Lattanzio, V. (2009). A
460 reproducible, rapid and inexpensive Folin-Ciocalteu micro-method in determining
461 phenolics of plant methanol extracts. *Microchemical Journal*, 91(1), 107–110.
462 <https://doi.org/10.1016/j.microc.2008.08.011>

463 Davis, T., Llanes, F., Volesky, B., & Mucci, A. (2003). Metal selectivity of *Sargassum spp.*
464 and their alginates in relation to α -L-guluronic acid content and conformation.
465 *Environmental Science & Technology*, 37, 261–267.
466 <https://doi.org/10.1021/es025781d>

467 DuBois, Michel., Gilles, K. A., Hamilton, J. K., Rebers, P. A., & Smith, F. (1956).
468 Colorimetric method for determination of sugars and related substances. *Analytical*
469 *Chemistry*, 28(3), 350–356. <https://doi.org/10.1021/ac60111a017>

- 470 Dusseault, J., Tam, S. K., Ménard, M., Polizu, S., Jourdan, G., Yahia, L., & Hallé, J.P. (2006).
471 Evaluation of alginate purification methods: Effect on polyphenol, endotoxin, and
472 protein contamination. *Journal of Biomedical Materials Research. Part A*, 76(2), 243–
473 251. <https://doi.org/10.1002/jbm.a.30541>
- 474 Fertah, M., Belfkira, A., Dahmane, E. Montassir, Taourirte, M., & Brouillette, F. (2017).
475 Extraction and characterization of sodium alginate from Moroccan
476 *Laminariadigitatabrown* seaweed. *Arabian Journal of Chemistry*, 10, S3707–S3714.
477 <https://doi.org/10.1016/j.arabjc.2014.05.003>
- 478 García-Ríos, V., Ríos-Leal, E., Robledo, D., & Freile-Pelegrin, Y. (2012). Polysaccharides
479 composition from tropical brown seaweeds. *Phycological Research*, 60(4), 305–315.
480 <https://doi.org/10.1111/j.1440-1835.2012.00661.x>
- 481 Gómez Ordóñez, E., & Rupérez, P. (2011). FTIR-ATR spectroscopy as a tool for
482 polysaccharide identification in edible brown and red seaweeds. *Food Hydrocolloids*,
483 25(6), 1514–1520. <https://doi.org/10.1016/j.foodhyd.2011.02.009>
- 484 Handå, A., Forbord, S., Wang, X., Broch, O. J., Dahle, S. W., Størseth, T. R., Reitan, K. I.,
485 Olsen, Y., & Skjermo, J. (2013). Seasonal- and depth-dependent growth of cultivated
486 kelp (*Saccharinalatissima*) in close proximity to salmon (*Salmo salar*) aquaculture in
487 Norway. *Aquaculture*, 414, 191–
488 201. <https://doi.org/10.1016/j.aquaculture.2013.08.006>
- 489
- 490 Hentati, F., Delattre, C., Ursu, A. V., Desbrières, J., Le Cerf, D., Gardarin, C., Abdelkafi, S.,
491 Michaud, P., & Pierre, G. (2018). Structural characterization and antioxidant activity
492 of water-soluble polysaccharides from the Tunisian brown seaweed
493 *Cystoseira compressa*. *Carbohydrate Polymers*, 198, 589–600.
494 <https://doi.org/10.1016/j.carbpol.2018.06.098>

495 Hentati, F., Pierre, G., Ursu, A. V., Vial, C., Delattre, C., Abdelkafi, S., & Michaud, P.
496 (2020). Rheological investigations of water-soluble polysaccharides from the Tunisian
497 brown seaweed *Cystoseira compressa*. *Food Hydrocolloids*, *103*, 105631.
498 <https://doi.org/10.1016/j.foodhyd.2019.105631>

499 Idris, S. S., Rahman, N. A., & Ismail, K. (2012). Combustion characteristics of Malaysian oil
500 palm biomass, sub-bituminous coal and their respective blends via thermogravimetric
501 analysis (TGA). *Bioresource Technology*, *123*, 581–591.
502 <https://doi.org/10.1016/j.biortech.2012.07.065>

503 Li, J., He, J., & Huang, Y. (2016). Role of alginate in antibacterial finishing of textiles.
504 *International Journal of Biological Macromolecules*, *94*(Pt A), 466–473.
505 <https://doi.org/10.1016/j.ijbiomac.2016.10.054>

506 Kahl, R., & Kappus, H. (1993). Toxikologie der synthetischen Antioxidantien BHA und BHT
507 im Vergleich mit dem natürlichen Antioxidans Vitamin E. *Zeitschrift für Lebensmittel-*
508 *Untersuchung und Forschung*, *196*(4), 329–338. <https://doi.org/10.1007/BF01197931>

509 Kardosová, A., & Machová, E. (2006). Antioxidant activity of medicinal plant
510 polysaccharides. *Fitoterapia*, *77*(5), 367–
511 373. <https://doi.org/10.1016/j.fitote.2006.05.001>

512 Kelishomi, Z. H., Goliaei, B., Mahdavi, H., Nikoofar, A., Rahimi, M., Moosavi-Movahedi, A.
513 A., Mamashli, F., & Bigdeli, B. (2016). Antioxidant activity of low molecular weight
514 alginate produced by thermal treatment. *Food Chemistry*, *196*, 897–902.
515 <https://doi.org/10.1016/j.foodchem.2015.09.091>

516 Kirby, A. J., & Schmidt, R. J. (1997). The antioxidant activity of Chinese herbs for eczema
517 and of placebo herbs — I. *Journal of Ethnopharmacology*, *56*(2), 103–108.
518 [https://doi.org/10.1016/s0378-8741\(97\)01510-9](https://doi.org/10.1016/s0378-8741(97)01510-9)

519 Kumar, P., Pawaria, S., Dalal, J., Ravesh, S., Bharadwaj, S., Jerome, A., Kumar, D., Jan, M.
520 H., & Yadav, P. S. (2019). Sodium alginate potentiates antioxidants, cryoprotection
521 and antibacterial activities of egg yolk extender during semen cryopreservation in
522 buffalo. *Animal Reproduction Science*, 209, 106166.
523 <https://doi.org/10.1016/j.anireprosci.2019.106166>

524 Kumar, S., & Sahoo, D. (2017). A comprehensive analysis of alginate content and biochemical
525 composition of leftover pulp from brown seaweed *Sargassum wightii*. *Algal Research*,
526 23, 233–239. <https://doi.org/10.1016/j.algal.2017.02.003>

527 Larsen, B., Salem, D. M. S. A., Sallam, M. A. E., Mishrikey, M. M., & Beltagy, A. I. (2003).
528 Characterization of the alginates from algae harvested at the Egyptian Red Sea coast.
529 *Carbohydrate Research*, 338(22), 2325–2336. [https://doi.org/10.1016/s0008-](https://doi.org/10.1016/s0008-6215(03)00378-1)
530 [6215\(03\)00378-1](https://doi.org/10.1016/s0008-6215(03)00378-1)

531 Liu, S., Liu, G., & Yi, Y. (2015). Novel vanadyl complexes of alginate saccharides:
532 Synthesis, characterization, and biological activities. *Carbohydrate Polymers*, 121,
533 86–91. <https://doi.org/10.1016/j.carbpol.2014.11.069>

534 Liu, Z.Q. (2020). Bridging free radical chemistry with drug discovery: A promising way for
535 finding novel drugs efficiently. *European Journal of Medicinal Chemistry*, 189,
536 112020. <https://doi.org/10.1016/j.ejmech.2019.112020>

537 López-González, D., Fernandez-Lopez, M., Valverde, J. L., & Sanchez-Silva, L. (2014).
538 Pyrolysis of three different types of microalgae: Kinetic and evolved gas analysis.
539 *Energy*, 73(C), 33–43.

540 Lorenzo, J. M., González-Rodríguez, R. M., Sánchez, M., Amado, I. R., & Franco, D. (2013).
541 Effects of natural (grape seed and chestnut extract) and synthetic antioxidants
542 (butylated hydroxytoluene, BHT) on the physical, chemical, microbiological and

543 sensory characteristics of dry cured sausage “chorizo.” *Food Research International*,
544 54(1), 611–620. <https://doi.org/10.1016/j.foodres.2013.07.064>

545 Mallick, D., Poddar, M. K., Mahanta, P., & Moholkar, V. S. (2018). Discernment of
546 synergism in pyrolysis of biomass blends using thermogravimetric analysis.
547 *Bioresource Technology*, 261, 294–305.
548 <https://doi.org/10.1016/j.biortech.2018.04.011>

549 Mohammed, A., Rivers, A., Stuckey, David. C., & Ward, K. (2020). Alginate extraction from
550 *Sargassum* seaweed in the Caribbean region: Optimization using response surface
551 methodology. *Carbohydrate Polymers*, 245, 116419.
552 <https://doi.org/10.1016/j.carbpol.2020.116419>

553 Morris, E. R., Rees, D. A., & Thom, D. (1980). Characterisation of alginate composition and
554 block-structure by circular dichroism. *Carbohydrate Research*, 81(2), 305–314.
555 [https://doi.org/10.1016/S0008-6215\(00\)85661-X](https://doi.org/10.1016/S0008-6215(00)85661-X)

556 Okolie, C. L., Mason, B., Mohan, A., Pitts, N., & Udenigwe, C. C. (2020). Extraction
557 technology impacts on the structure-function relationship between sodium alginate
558 extracts and their *in vitro* prebiotic activity. *Food Bioscience*, 37, 100672.
559 <https://doi.org/10.1016/j.fbio.2020.100672>

560 Parthiban, C., Parameswari, K., Saranya, C., Hemalatha, A., & Anantharaman, P. (2012).
561 Production of sodium alginate from selected seaweeds and their physiochemical and
562 biochemical properties. *Asian Pacific Journal of Tropical Biomedicine*, 1, 1–4.

563 Pellegrini, M., Valls, R., & Pellegrini, L. (1997). *Chimiotaxonomie et marqueurs chimiques*
564 *dans les algues brunes. Lagasalia*, 19, 145–164.
565 <https://idus.us.es/xmlui/handle/11441/63026>

566 Ramos, P. E., Silva, P., Alario, M. M., Pastrana, L. M., Teixeira, J. A., Cerqueira, M. A., &
567 Vicente, A. A. (2018). Effect of alginate molecular weight and M/G ratio in beads

568 properties foreseeing the protection of probiotics. *Food Hydrocolloids*, 77, 8–16.
569 <https://doi.org/10.1016/j.foodhyd.2017.08.031>

570 Raza, W., Makeen, K., Wang, Y., Xu, Y., & Qirong, S. (2011). Optimization, purification,
571 characterization and antioxidant activity of an extracellular polysaccharide produced
572 by *Paenibacilluspolymyxa* SQR-21. *Bioresource Technology*, 102(10), 6095–6103.
573 <https://doi.org/10.1016/j.biortech.2011.02.033>

574 Rengasamy, K. R., Mahomoodally, M. F., Aumeeruddy, M. Z., Zengin, G., Xiao, J., & Kim,
575 D. H. (2020). Bioactive compounds in seaweeds: An overview of their biological
576 properties and safety. *Food and Chemical Toxicology*, 135, 111013.
577 <https://doi.org/10.1016/j.fct.2019.111013>

578 Rezende, R. A., Bártolo, P. J., Mendes, A., & Filho, R. M. (2009). Rheological behavior of
579 alginate solutions for biomanufacturing. *Journal of Applied Polymer Science*, 113(6),
580 3866–3871. <https://doi.org/10.1002/app.30170>

581 Sanjeeva, K. K. A., Lee, J. S., Kim, W. S., & Jeon, Y. J. (2017). The potential of brown-algae
582 polysaccharides for the development of anticancer agents: An update on anticancer
583 effects reported for fucoidan and laminaran. *Carbohydrate Polymers*, 177, 451–459.
584 <https://doi.org/10.1016/j.carbpol.2017.09.005>

585 Schramm, D. D., Karim, M., Schrader, H. R., Holt, R. R., Cardetti, M., & Keen, C. L. (2003).
586 Honey with high levels of antioxidants can provide protection to healthy human
587 subjects. *Journal of Agricultural and Food Chemistry*, 51(6), 1732–1735.
588 <https://doi.org/10.1021/jf025928k>

589 Scott, R. W. (1979). Colorimetric determination of hexuronic acids in plant materials.
590 *Analytical Chemistry*, 51(7), 936–941. <https://doi.org/10.1021/ac50043a036>

591 Sellimi, S., Younes, I., Ayed, H. B., Maalej, H., Montero, V., Rinaudo, M., Dahia, M.,
592 Mechichi, T., Hajji, M., & Nasri, M. (2015). Structural, physicochemical and

593 antioxidant properties of sodium alginate isolated from a Tunisian brown seaweed.
594 *International Journal of Biological Macromolecules*, 72, 1358–1367.
595 <https://doi.org/10.1016/j.ijbiomac.2014.10.016>

596 Setyawidati, N. A. R., Puspita, M., Kaimuddin, A. H., Widowati, I., Deslandes, E.,
597 Bourgougnon, N., & Stiger-Pouvreau, V. (2018). Seasonal biomass and alginate stock
598 assessment of three abundant genera of brown macroalgae using multispectral high
599 resolution satellite remote sensing: A case study at Ekas Bay (Lombok, Indonesia).
600 *Marine Pollution Bulletin*, 131, 40–48.
601 <https://doi.org/10.1016/j.marpolbul.2017.11.068>

602 Shang, H., Zhou, H., Duan, M., Li, R., Wu, H., & Lou, Y. (2018). Extraction condition
603 optimization and effects of drying methods on physicochemical properties and
604 antioxidant activities of polysaccharides from comfrey (*Symphytum officinale* L.) root.
605 *International Journal of Biological Macromolecules*, 112, 889–899.
606 <https://doi.org/10.1016/j.ijbiomac.2018.01.198>

607 Suzuki, S., Ono, M., Toda, T., & Kitamura, S. (2016). Preparation and intestinal
608 immunostimulating activity of low molecular weight alginate from *Saccharina*
609 (*Laminaria*) species in Japan. *Journal of Applied Glycoscience*, 63(1), 1–5.
610 https://doi.org/10.5458/jag.jag.JAG-2015_017

611 Wang, J., Hu, S., Nie, S., Yu, Q., & Xie, M. (2016). Reviews on mechanisms of *in*
612 *vitro* antioxidant activity of polysaccharides. *Oxidative Medicine and Cellular*
613 *Longevity*.2016, Article ID 5692852, 13 pages. <https://doi.org/10.1155/2016/5692852>

614 Xiao, Q., Tong, Q., Zhou, Y., & Deng, F. (2015). Rheological properties of pullulan-sodium
615 alginate based solutions during film formation. *Carbohydrate Polymers*, 130, 49–56.
616 <https://doi.org/10.1016/j.carbpol.2015.04.069>

617 Yang, J.S., Xie, Y.J., & He, W. (2011). Research progress on chemical modification of
618 alginate: A review. *Carbohydrate Polymers*.84(1), 33–39.[http://agris.fao.org/agris-](http://agris.fao.org/agris-search/search.do?recordID=US201600049890)
619 [search/search.do?recordID=US201600049890](http://agris.fao.org/agris-search/search.do?recordID=US201600049890)

620 Yildirim, A., Mavi, A., & Kara, A. A. (2001). Determination of antioxidant and antimicrobial
621 activities of *Rumexcrispus*L. extracts. *Journal of Agricultural and Food Chemistry*,
622 49(8), 4083–4089.

623 Zhao, D., Xu, J., & Xu, X. (2018). Bioactivity of fucoidan extracted from *Laminaria japonica*
624 using a novel procedure with high yield. *Food Chemistry*, 245, 911–918.
625 <https://doi.org/10.1016/j.foodchem.2017.11.083>

626 Zhu, Y., Wu, L., Chen, Y., Ni, H., Xiao, A., &Cai, H. (2016). Characterization of an
627 extracellular biofunctional alginate lyase from marine *Microbulbifer sp.* ALW1 and
628 antioxidant activity of enzymatic hydrolysates. *Microbiological Research*, 182, 49–58.
629 <https://doi.org/10.1016/j.micres.2015.09.004>

630
631
632

633 **Table 1.** Extraction yield(g/100 g DM) and chemical composition (g/100 g DM) of the CSSA
 634 fractions from different seasons.

Parameters	Season			
	AD	AA	AJ	AS
639 Yield	25.1±0.4 ^c	28±1 ^b	38.4±0.3 ^a	21±1 ^d
640 Moisture*	11.3±0.1 ^b	10.0±0.4 ^c	10±0.5 ^d	12.6±0.4 ^a
641 Neutral sugars	9.2±0.4 ^a	6.3±0.4 ^b	5.5±0.4 ^c	6.1±0.3 ^b
642 Uronic acids	47±1 ^d	53±2 ^c	66±2 ^a	62±1 ^b
643 Total phenolics‡	1.47±0.01 ^a	1.03±0.02 ^b	0.92±0.01 ^c	0.66±0.02 ^d
644 Ash	39.4±0.1 ^a	37±0.5 ^b	24.3±0.4 ^d	29±1 ^c
645 C	35±2 ^b	40±1 ^a	28±1 ^c	39.6±0.3 ^a
646 O	45.4±0.1 ^a	43±2 ^b	41±1 ^c	46±1 ^a
647 Na	16±1 ^b	14.9±0.4 ^b	26±1 ^a	10.5±0.3 ^c
648 S	0	0	0	0
649 N	0	0	0	0
650 Mg	0	0.17±0.01 ^c	0.25±0.01 ^b	0.44±0.03 ^a
651 K	0.18±0.01 ^c	0.53±0.01 ^a	0.44±0.04 ^b	0.17±0.01 ^c
652 Cl	0.39±0.01 ^b	1.24±0.1 ^a	0.35±0.04 ^b	1.38±0.1 ^a
653 Si	0.36±0.08 ^b	0.27±0.01 ^c	0.57±0.05 ^a	0.26±0.02 ^c

661 AD, AA, AJ and AS represent sodium alginates extracted from *C. schiffneri* collected in December, April, July
 662 and September, respectively; *The moisture is expressed as g/100 g lyophilized sodium alginate;‡Total
 663 phenolics were expressed as g eq. phloroglucinol/100 g DM; Each value represents the mean±SD (*n* = 3);
 664 ^{a,b,c,d}Different letters within different seasons of harvest (same column) indicate significant differences (*p*<0.05).

665
 666

667 **Table 2.** M/G ratios of the CSSA fractions from different seasons.

Method	Season			
	AD	AA	AJ	AS
FTIR	0.062	0.064	0.065	0.062
Circular dichroism	0	0.022	0.012	0.015
NMR	0.093	0.024	0.037	0.080

668 AD, AA, AJ and AS represent sodium alginates extracted from *C. schiffneri* collected in December, April, July
669 and September, respectively.

670

671 **Table 3.** Average molecular mass (g/mol) of the CSSA fractions from different seasons.

	Season			
	AD	AA	AJ	AS
M_n	7.62×10 ⁵	8.02×10 ⁴	1.26×10 ⁵	7.85×10 ²
M	1.23×10 ⁶	1.16×10 ⁵	2.33×10 ⁵	4.49×10 ³
PDI	1.62	1.45	1.85	5.72

672 AD, AA, AJ and AS represent sodium alginates extracted from *C. schiffneri* collected in December, April, July
673 and September, respectively; M_n, M, and PDI are the number-average molecular mass, the average molecular
674 mass, and the polydispersity index, respectively.

675

676

677

678

679

680 **Table4.**Structural composition of the CSSA fractions from different seasons.

Season	F_G	F_M	F_{GG}	F_{MM}	F_{MG}	F_{GM}
AD	0.91	0.09	0.88	0.06	0.03	0.03
AA	0.98	0.02	0.97	0.01	0.01	0.01
AJ	0.97	0.03	0.96	0.02	0.01	0.01
AS	0.92	0.08	0.9	0.06	0.02	0.02

681 AD, AA, AJ and AS represent sodium alginates extracted from *C. schiffneri* collected in December, April, July
682 and September, respectively.

683

684 **Table 5.** Antioxidant activities of the CSSA fractions from different seasons.

685

	Season				Standards	
	AD	AA	AJ	AS	BHA	EDTA
DPPH•						
scavenging activity	>1500	>1500	>1500	190±10 ^a	14.1±0.2 ^b	
Reducing power	51±1 ^b	>500	208±6 ^a	51±2 ^b	25.2±0.1 ^c	
Fe²⁺chelating ability	145±1 ^c	511±17 ^a	211±6 ^b	43±1 ^d		10.0±0.2 ^e

686 AD, AA, AJ and AS represent sodium alginates extracted from *C. schiffneri* collected in December, April, July
 687 and September, respectively; Results of DPPH• scavenging and metal (Fe²⁺) chelating assays are shown as
 688 IC₅₀ values (µg/ml), defined as the extract concentration needed to scavenge 50% of DPPH• and to chelate 50%
 689 of Fe²⁺, respectively. The reducing power (OD 700) is shown as the extract concentration (EC_{0.5}) providing 0.5
 690 absorbance at 700 nm; Each value represents the mean±SD (*n* = 3); ^{a,b,c,d,e} Different letters within different
 691 seasons of harvest (same row) indicate significant differences (*p*<0.05).
 692

693 **Figure captions**

694 **Fig. 1.** ATR-FTIR spectroscopy of sodium alginates extracted from *C. schiffneri* collected in
695 December (AD), April (AA), July (AJ) and September (AS).

696 **Fig. 2.** Circular dichroism spectra of sodium alginates extracted from *C. schiffneri* collected in
697 December (AD), April (AA), July (AJ) and September (AS).

698 **Fig. 3.** ¹H-NMR spectra of sodium alginates extracted from *C. schiffneri* collected in
699 December (AD), April (AA), July (AJ) and September (AS).

700 **Fig. 4.** Thermogravimetric analysis of sodium alginates extracted from *C. schiffneri* collected
701 in December (AD), April (AA), July (AJ) and September (AS).

702 **Fig. 5.** Viscosity of sodium alginates extracted from *C. schiffneri* collected in December
703 (AD), April (AA), July (AJ) and September (AS).

704 **Fig. 6.** Viscoelasticity of sodium alginates extracted from *C. schiffneri* collected in December
705 (AD), April (AA), July (AJ) and September (AS).

706 **Fig. 7.** Antioxidant activities of sodium alginates extracted from *C. schiffneri* collected in
707 December (AD), April (AA), July (AJ) and September (AS).

708

709 **Fig. 1.**

710

711

712

713

714

715

716

717

718

719

720

721

722

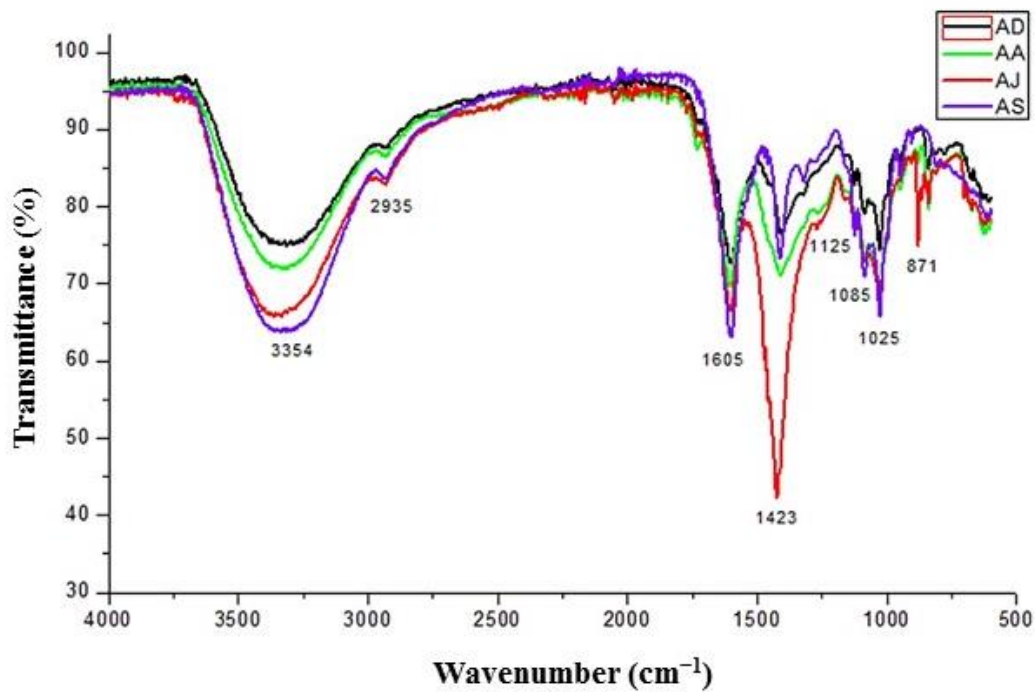
723

724

725

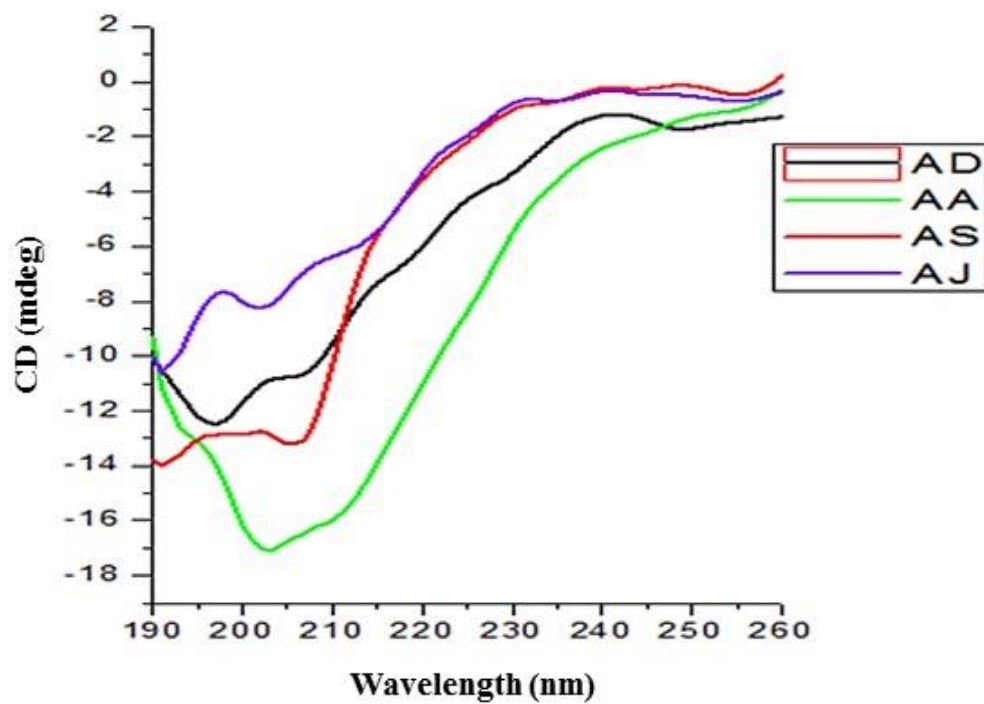
726

727



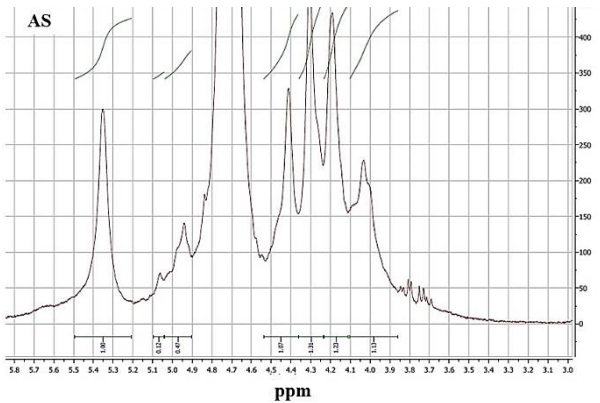
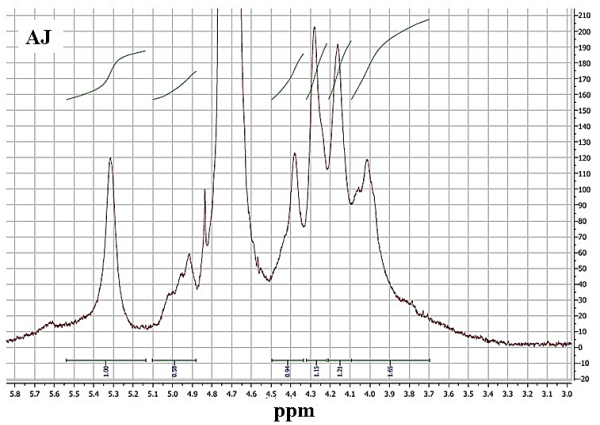
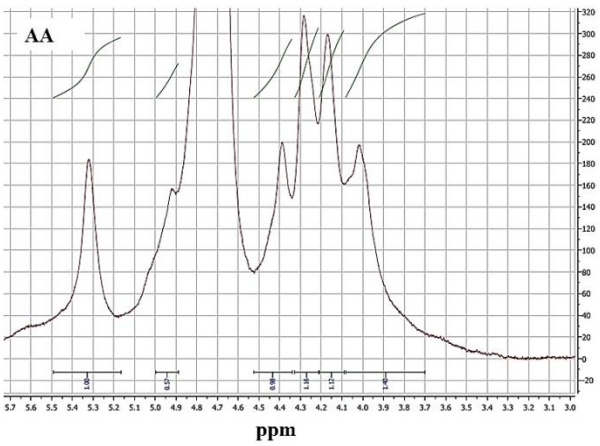
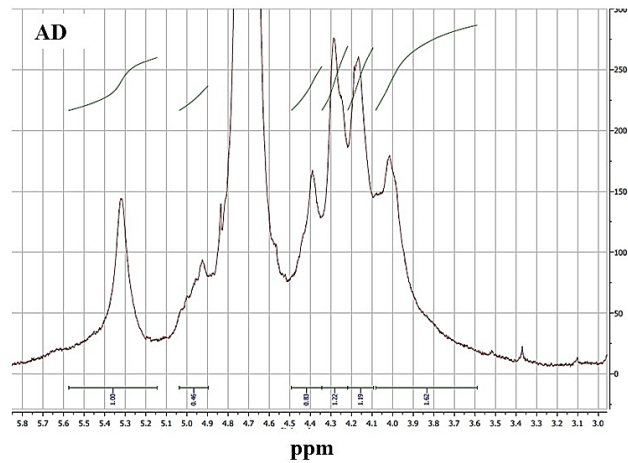
728 **Fig. 2.**

729
730
731
732
733
734
735
736
737
738
739
740
741
742
743
744
745



746 **Fig. 3.**

747
748
749
750
751
752
753
754
755
756
757
758
759
760
761
762
763
764
765
766
767
768
769
770
771
772
773
774
775
776
777
778
779
780
781
782
783
784
785
786
787
788



789 **Fig. 4.**

790

791

792

793

794

795

796

797

798

799

800

801

802

803

804

805

806

807

808

809

810

811

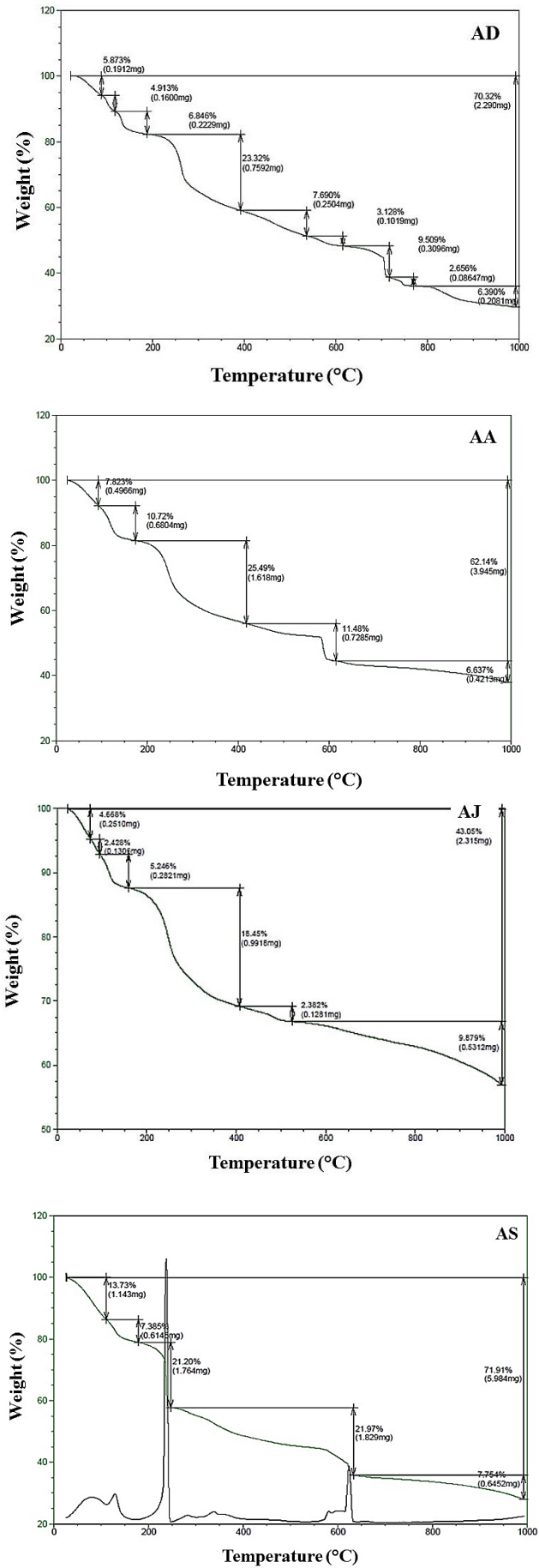
812

813

814

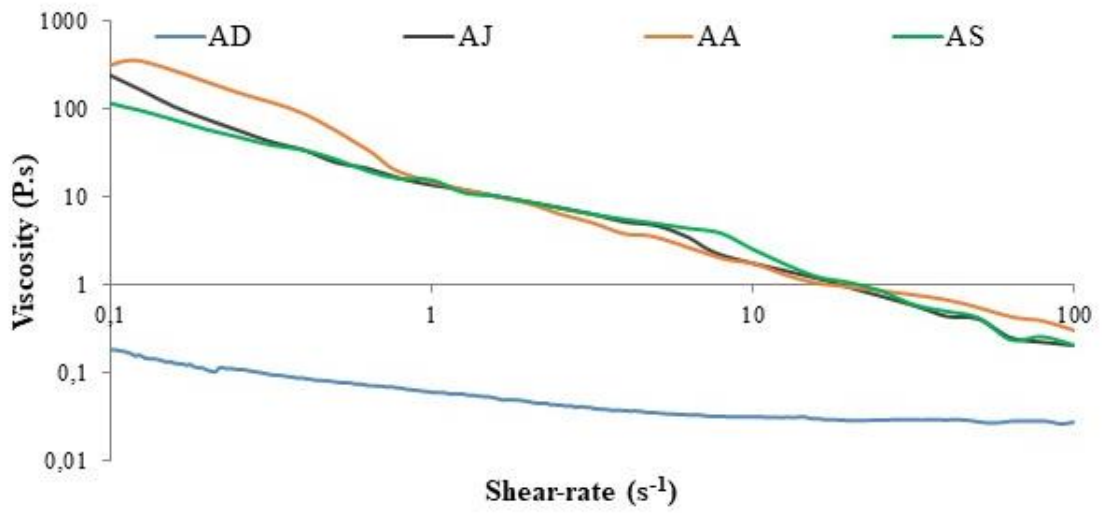
815

816



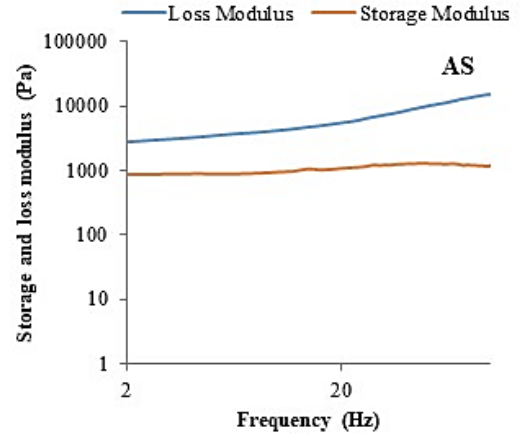
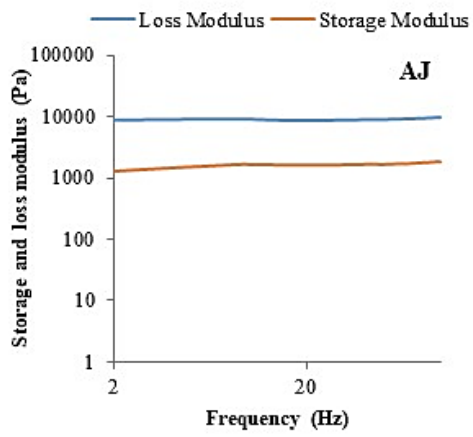
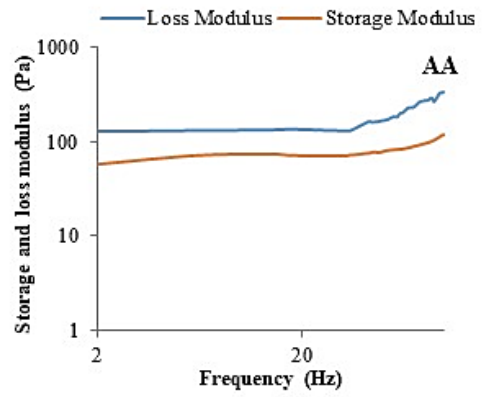
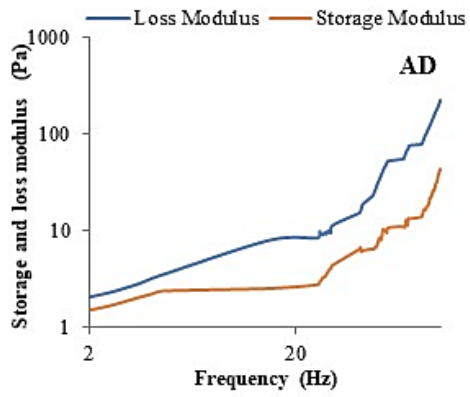
817 **Fig. 5.**

818
819
820
821
822
823
824
825
826
827
828
829
830
831
832
833
834
835
836
837



838 **Fig. 6.**

839
840
841
842
843
844
845
846
847
848
849
850
851
852
853
854
855
856
857
858
859
860
861
862



863 Fig. 7.

864
865
866
867
868
869
870
871
872
873
874
875
876
877
878
879
880
881
882
883
884
885
886
887
888
889
890
891
892
893
894
895
896
897
898
899
900
901
902
903
904

